

On the stochastic engine of transmittable diseases in exponentially growing populations

Torsten Lindström

Department of Mathematics
Linnæus University
SE-35195 Växjö, SWEDEN

Abstract

The purpose of this paper is to analyze the interplay of deterministic and stochastic models for epidemic diseases. Deterministic models for epidemic diseases are prone to predict global stability. If the natural birth and death rates are assumed small in comparison to disease parameters like the contact rate and the recovery rate, then the globally stable endemic equilibrium corresponds to a tiny proportion of infected individuals. Asymptotic equilibrium levels corresponding to low numbers of individuals invalidate the deterministic results.

Diffusion effects force frequency functions of the stochastic model to possess similar stability properties as the deterministic model. Particular simulations of the stochastic model are, however, oscillatory and predict oscillatory patterns. Smaller or isolated populations show longer periods, more violent oscillations, and larger probabilities of extinction.

We prove that evolution maximizes the infectiousness of the disease as measured by the ability to increase the proportion of infected individuals. This hold provided the stochastic oscillations are moderate enough to remain in the vicinity of the deterministic equilibrium.

We close our paper with a discussion of the herd-immunity concept and stress its close relation to vaccination-campaigns.

1 Introduction

Many properties of the epidemic bell-shaped curve have been known since Kermack and McKendrick (1927). Their first result was that there exists a threshold density of susceptible individuals such that if the density of susceptible individuals exceeds that threshold, then there will be an epidemic. They used the term excess to describe the difference between the density of susceptible individuals and the threshold density. Their second result states that if the excess is small, then the epidemic curve is symmetric and the eventual number of ill corresponds to the double of the excess. Such results do not hold for large excesses but their third result states that a very infectious disease exhausts almost the whole population of susceptible individuals. The general result is that the eventual number of ill is an increasing function of the infectiousness of the disease.

The most well-known measure of the infectiousness of a disease is R_0 . It is a dimensionless quantity giving the number of secondary infections resulting from each infection in an entirely susceptible population. In many cases, it is the product of the contact rate and the time spent by an infected individual in the population. Evolution of diseases tends to increase a parameter that is closely related to R_0 , see Section 4. In order to increase the time that an infected individual spends in the population, diseases are expected to become less virulent with time. However, it is the product R_0 that is maximized, not the contact rate nor the time in the population. If evolutionary changes that allows an increased contact rate are available, then the pathogen do not need to become less virulent.

Many pre-vaccination pandemic mitigation strategies (lock-downs, social distancing, testing, contact tracing, and quarantine restrictions) aim at making the disease less infectious and hence to decrease R_0 . Kermack and McKendrick (1927) predicts that the eventual number of ill decreases as such measures are applied. Testing, contact tracing and quarantine restrictions removes infected individuals from the population and thus, decrease the time spent by an infected individual in the population. Such measures are specific in the sense that they attack a selected specific pathogen. The drawback with these measures is that their efficiency drops rapidly with the size of the epidemic and that a surplus of technical equipment and medical competence do not exist in the beginning of a new pandemic.

Lock-downs and social distancing are general measures that can be applied if the epidemic has grown too large. They do not possess the capacity

and competence bottlenecks mentioned above but their drawback are the huge costs on society level limiting the time such strategies can be applied. In the huge cities there are also bottleneck problems as stairs, elevators and almost no real possibility to move efficiently without public transportation etc. that decrease the possibilities of implementing any lock-downs efficiently over longer periods. Their objective must be to increase the contact-tracing and testing capacity considerably in order to preserve R_0 afterwards. All mitigation strategies do not have an impact on R_0 alone. Regional quarantine and travel restrictions are such examples. Apart from having an impact on the contact rate, they split the population into smaller units magnifying the probability of extinction of the disease.

Germann, Kadau, Longini, and Macken (2006) criticized the classical results and concluded that some of the mitigation strategies does just delay the pandemic without affecting the eventual number of ill. We suspect that these simulation results have never been validated against Kermack and McKendrick (1927) in limiting cases. A far more severe criticism against the classical models is their tendency to predict global stability in contrast to the outbreaks that usually are observed. It is often concluded that these global stability properties of epidemic models are extremely robust. Delays have been considered as sources of instabilities for a large number of systems (see e. g. Smith (2011)) but they are not in general sources of instabilities for epidemic models (McCluskey (2010)).

Another possible source of instability is the seasonality of the disease. There is substantial evidence for that many pathogens are more infectious during certain seasons (may be wet, dry, cold, humid, or hot seasons). Evidence for period doubling routes to chaos (Glendinning and Perry (1997), Keeling, Rohani, and Grenfell (2001), and Olsen and Schaffer (1990)) and deterministic chaos (Barrentos, Ángel-Rodríguez, and Ruiz-Herrera (2017)) connected to seasonal epidemic models exists.

A dominant pattern in all epidemic oscillations is, however, the tendency to display more erratic patterns with a lower mean number of cases and more isolated populations. More erratic patterns with lower mean numbers of cases are e. g. a dominating pattern in the measles, whooping coach, and rubella data used in Keeling, Rohani, and Grenfell (2001). More evidence is obtained when comparing long term measles data before the vaccination era in London (Becker, Wesolowski, Bjørnstad, and Grenfell (2019)) to the more isolated population at Iceland (Cliff and Haggett (1980)). Deterministic representations of birth-death processes (Bailey (1964)) remain less valid for

smaller populations.

The second serious problem with many epidemiological models is the lack of structural stability, cf. Guckenheimer and Holmes (1983). This is a problem is visible already in the models by Kermack and McKendrick (1927). The characteristic of a structurally unstable model is that its predictions are sensitive to various assumptions done in the model. One example is the bell-shaped epidemic curve mentioned above. It has the tendency to approach zero both before and after its maximum giving the impression that an epidemic does not remain in the population after invading it despite the above-mentioned global stability results.

Our approach to remedy the structural stability problem is to consider an epidemic model allowing for exponential growth of the population. In order to make sure that our analysis can be made on a compact set, a transformation to density variables is done. For most diseases, the natural birth and death parameters tend to operate on a slower scale than typical disease parameters like the contact rate and the recovery rate. After an epidemic this parameter asymmetry forces the number of infected individuals to low numbers making differential equations approximations of birth-death processes (Bailey (1964)) invalid. Several models that we encounter have neither been formulated nor been well-studied before. This constitutes a mechanism for the observed instabilities and explains why not only the disease parameters but also the population size plays an important role as a source of instability for infectious diseases.

The structure of our paper is as follows: We formulate the deterministic version of the model in Section 2. We list basic properties of stochastic models in Section 2, too. We make a transition to density coordinates for the deterministic model in Section 3. This guarantees the existence of a compact invariant set for the deterministic model. We consider the evolutionary development of the involved pathogens in Section 4 and prove a global stability theorem. We discuss dimensionless parameters in Section 5 and follow up with a discussion of relations between the involved parameters and their consequences for the application of various pandemic mitigation strategies in Section 6. We formulate the complete stochastic version of the model in Section 7. We analyze it numerically in a number of ways and compare the results to the deterministic damped oscillations. In Section 8, we discuss vaccination campaigns and their close relation to the herd-immunity concept. Section 9 contains a summary of our results.

2 The model

We consider the following system of nonlinear ordinary differential equations

$$\begin{aligned}\dot{S} &= \lambda N - \beta_1 S \frac{I_1}{N} - \beta_2 S \frac{I_2}{N} - \mu S, \\ \dot{I}_1 &= \beta_1 S \frac{I_1}{N} - \gamma_1 I_1 - \mu I_1, \\ \dot{I}_2 &= \beta_2 S \frac{I_2}{N} - \gamma_1 I_2 - \mu I_2, \\ \dot{R} &= \gamma_1 I_1 + \gamma_2 I_2 - \mu R.\end{aligned}\tag{1}$$

and its corresponding stochastic counterparts. Its variables are S , the number of susceptible individuals, I_1 , the number individuals infected with strain 1, I_2 , the number individuals infected with strain 2, and finally, R , the number of recovered. The recovered individuals may consist of either immune individuals or infected individuals in quarantine. In this way a more appropriate term for these individuals could be removed individuals. The parameters are the birth rate λ , the contact rate β_1 for strain 1, the contact rate β_2 for strain 2, the mortality μ , the recovery rate γ_1 for strain 1, and the recovery rate γ_2 for strain 2. We consider neither the possibility of coinfection with both strains nor the possibility of an excess mortality due to any or both of the infections. The reason is that this assumption gives a prototype case allowing for a more precise analysis that can be used for validation of simulations. In this case, the whole population grows exponentially since

$$\dot{N} = \dot{S} + \dot{I}_1 + \dot{I}_2 + \dot{R} = \lambda N - \mu S - \mu I_1 - \mu I_2 - \mu R = (\lambda - \mu)N,\tag{2}$$

with $N(0) = N_0$. Therefore, we have for the whole population $N(t) = N_0 \exp((\lambda - \mu)t)$.

We shall consider the deterministic model (1) side by side with its stochastic counterparts. The corresponding stochastic model for the whole population is well known, see e. g. Bailey (1964). Indeed, consider the corresponding birth-death Markov process with state space $\mathbf{N} = \{0, 1, 2, \dots\}$. Let $p_N(t)$ be the probability that the population size is N at time t . We assume that

$$\begin{aligned}\text{Chance of one birth} &= \lambda N(t)\delta t + o(t), \\ \text{Chance of one death} &= \mu N(t)\delta t + o(t), \\ \text{Chance of more than one death/birth} &= o(t).\end{aligned}$$

The differential-difference equations

$$\begin{aligned}\dot{p}_N &= \lambda(N-1)p_{N-1} - (\lambda + \mu)Np_N + \mu(N+1)p_{N+1}, \quad N = 1, 2, 3 \dots \\ \dot{p}_0 &= \mu p_1\end{aligned}\tag{3}$$

on \mathbf{R}^∞ gives the probabilities that the population has a given size at time t . If we know that the initial population size is N_0 , then $p_{N_0}(0) = 1$ and $p_N(0) = 0$ for $N \neq N_0$. Bailey (1964) proved that (3) has the solution

$$\begin{aligned}p_N(t) &= \sum_{j=0}^{\min(N_0, N)} \binom{N_0}{j} \binom{N_0 + N - j - 1}{N_0 - 1} \alpha^{N_0 - j} \beta^{N - j} (1 - \alpha - \beta)^j, \\ p_0(t) &= \alpha^{N_0}, \\ \text{with } \alpha &= \frac{\mu(1 - e^{-(\lambda - \mu)t})}{\lambda - \mu e^{-(\lambda - \mu)t}} \quad \text{and} \quad \beta = \frac{\lambda(1 - e^{-(\lambda - \mu)t})}{\lambda - \mu e^{-(\lambda - \mu)t}}\end{aligned}\tag{4}$$

The extinction state containing zero individuals is an absorbing state indicated by the fact that the probability of extinction increases with time. The eventual probability of extinction equals one if $\lambda \leq \mu$ and is $(\mu/\lambda)^{N_0}$ when $\lambda > \mu$. We conclude that the eventual probability of extinction decreases rapidly with initial population size if $\lambda > \mu$. We shall use the above results for the validation of our simulation results in limiting cases later on. Bailey (1964) also found that

$$\begin{aligned}E(N(t)|N(0) = N_0) &= N_0 \exp((\lambda - \mu)t) \\ V(N(t)|N(0) = N_0) &= \frac{N_0(\lambda + \mu)}{(\lambda - \mu)} \exp((\lambda - \mu)t) (\exp((\lambda - \mu)t) - 1)\end{aligned}$$

meaning that the expected value of the introduced stochastic process coincides with the deterministic value. Unfortunately, such nice results do not always hold in nonlinear cases.

In order to be well-formulated, the differential-difference equations (3) must keep the total probability invariant. This is easy to check for (3). We add the following lemma with proof because this turns out to be an important technique for checking the validity of more complicated sets of differential-difference equations later on.

Lemma 1. *The total probability $\sum_{N=0}^{\infty} p_N$ is an invariant for (3) and the total contribution to changes in the total probability that are related to each of the parameters are zero.*

Proof. We get

$$\begin{aligned}
\sum_{N=0}^{\infty} \frac{dp_N}{dt} &= \mu p_1 + \lambda \sum_{N=1}^{\infty} (N-1)p_{N-1} \\
&\quad - (\lambda + \mu) \sum_{N=1}^{\infty} Np_N + \mu \sum_{N=1}^{\infty} (N+1)p_{N+1} \\
&= \mu p_1 + \lambda \sum_{N=0}^{\infty} Np_N - \lambda \sum_{N=1}^{\infty} Np_N \\
&\quad - \mu \sum_{N=1}^{\infty} Np_N + \mu \sum_{N=2}^{\infty} Np_N = 0
\end{aligned}$$

and hence the total probability is invariant with respect to time. It is also instructive to divide the above computation into

$$\mu p_1 - \mu \sum_{N=1}^{\infty} Np_N + \mu \sum_{N=1}^{\infty} (N+1)p_{N+1} = 0$$

and

$$\lambda \sum_{N=1}^{\infty} (N-1)p_{N-1} - \lambda \sum_{N=1}^{\infty} Np_N = 0.$$

Therefore, the contributions to the changes in the total probability are zero for both the death and the birth process. \square

The interchange between the birth-death process (3) and the differential equation model (2) describes the transition from the stochastic dynamics that is governing for a small number of individuals to the approximating deterministic dynamics ruling a situation when the population is large and the probability of extinction remains negligible. It will be evident later, that both frameworks must be used for understanding the dynamics of infectious diseases. One of the objectives of this paper is to make the fundamental processes that force any epidemic into such a model interaction explicit.

3 A compact simplex

The exponential growth for (1) alluded to in Section 2 has a drawback. It does not ensure that the limit sets of all solutions are compact quantities.

This has the consequence that many statements regarding limit sets of the corresponding solutions would remain less precise. A transition to a density formulation will cure this problem since it will project all solutions to a compact simplex.

We introduce the density coordinates

$$x(t) = \frac{S(t)}{N(t)}, \quad y(t) = \frac{I_1(t)}{N(t)}, \quad z(t) = \frac{I_2(t)}{N(t)}, \quad u(t) = \frac{R(t)}{N(t)}$$

and get through the chain rule

$$\begin{aligned} \dot{x} &= \frac{\dot{S}N - S\dot{N}}{N^2(t)} = \frac{\lambda N^2 - \beta_1 S I_1 - \beta_2 S I_2 - \mu S N - S N (\lambda - \mu)}{N^2(t)} \\ &= \lambda - \beta_1 x y - \beta_2 x z - \mu x - (\lambda - \mu) x = \lambda - \lambda x - \beta_1 x y - \beta_2 x z, \\ \dot{y} &= \frac{\dot{I}_1 N - I_1 \dot{N}}{N^2(t)} = \frac{\beta_1 S I_1 - \gamma I_1 N - \mu I_1 N - I_1 N (\lambda - \mu)}{N^2(t)} \\ &= \beta_1 x y - \gamma_1 y - \mu y - (\lambda - \mu) y = \beta_1 x y - \gamma_1 y - \lambda y, \\ \dot{z} &= \frac{\dot{I}_2 N - I_2 \dot{N}}{N^2(t)} = \frac{\beta S I_2 - \gamma I_2 N - \mu I_2 N - I_2 N (\lambda - \mu)}{N^2(t)} \\ &= \beta_2 x z - \gamma_2 z - \mu z - (\lambda - \mu) z = \beta_2 x z - \gamma_2 z - \lambda z, \\ \dot{u} &= \frac{\dot{R} N - R \dot{N}}{N^2(t)} = \frac{\gamma_1 I_1 N + \gamma_2 I_2 N - \mu R N - R N (\lambda - \mu)}{N^2(t)} \\ &= \gamma_1 y + \gamma_2 z - \mu u - (\lambda - \mu) u = \gamma_1 y + \gamma_2 z - \lambda u. \end{aligned} \tag{5}$$

If we now add all equations, we get

$$\dot{x} + \dot{y} + \dot{z} + \dot{u} = \lambda - \lambda x - \lambda y - \lambda z - \lambda u = \lambda(1 - x - y - z - u). \tag{6}$$

Equation (6) implies that solutions starting at the simplex $x + y + z + u = 1$ remain at that simplex. That is, the simplex is an invariant compact set containing all solutions of interest for (5). Note that the natural mortality disappears from the model in its density formulation. Since the natural mortality removes infected individuals from the population R_0 cannot be a threshold parameter for (5) and we return later to the threshold parameters of the density formulated model. The reason is that R_0 expresses changes in the numbers of infected individuals and not changes in proportions of infected individuals.

Since $x(t) + y(t) + z(t) + u(t) = 1$, $\forall t \in \mathbf{R}$ we can still simplify our equations. It suffices to consider the first three equations, since the density of recovered is completely determined by those two equations. We get

$$\begin{aligned}\dot{x} &= \lambda - \lambda x - \beta_1 xy - \beta_2 xz = \beta_1 x \left(\frac{\lambda(1-x)}{\beta_1 x} - y \right) - \beta_2 xz, \\ &= f_i(x)F_i(x) - yf_1(x) - zf_2(x) \\ \dot{y} &= \beta_1 xy - \gamma_1 y - \lambda y = y\beta_1 \left(x - \frac{\gamma_1 + \lambda}{\beta_1} \right) = y\psi_1(x), \\ \dot{z} &= \beta_2 xz - \gamma_2 z - \lambda z = z\beta_2 \left(x - \frac{\gamma_2 + \lambda}{\beta_2} \right) = z\psi_2(x),\end{aligned}\tag{7}$$

with $f_i(x) = \beta_i x$, $F_i(x) = \lambda(1-x)/\beta_i x$, $\psi_i(x) = \beta_i x - \gamma_i - \lambda$, $i = 1, 2$. The introduced notation will save some work. The next theorem ensures that an infectious disease can never exhaust the whole population at the same time, a classical result that was already stated in Kermack and McKendrick (1927).

Theorem 1. *Put $\beta_* = \max(\beta_1, \beta_2)$. The tetrahedron $x \geq \lambda/\beta_*$, $x+y+z \leq 1$, $y \geq 0$, and $z \geq 0$ is an invariant compact set for (7).*

Proof. Solutions exist along the planes $y = 0$ and $z = 0$. Uniqueness of solutions ensure that no solutions can intersect these solutions. Moreover

$$\dot{x} + \dot{y} + \dot{z} = \lambda(1-x-y-z) - \gamma_1 y - \gamma_2 z < 0$$

whenever $x+y+z \geq 1$ and $y+z > 0$. Finally, we get with $\beta_* = \max(\beta_1, \beta_2)$,

$$\begin{aligned}\frac{dx}{dt} &= \lambda - \lambda x - \beta_1 xy - \beta_2 xz \geq \lambda - \lambda x - \beta_* x(1-x) \\ &= \lambda - \lambda x - \beta_* x + \beta_* x^2 = \lambda - (\lambda + \beta_*)x + \beta_* x^2 \\ &= \beta_* \left(x - \frac{\lambda}{\beta_*} \right) (x-1) \geq 0.\end{aligned}$$

Invariance follows. By being finite dimensional and closed and bounded it follows that the tetrahedron alluded to above is compact. \square

4 Global stability and evolutionary optimization

Model (7) contained two strains of the same disease with proportions y and z and we did not consider the possibility of coinfection of both strains. The

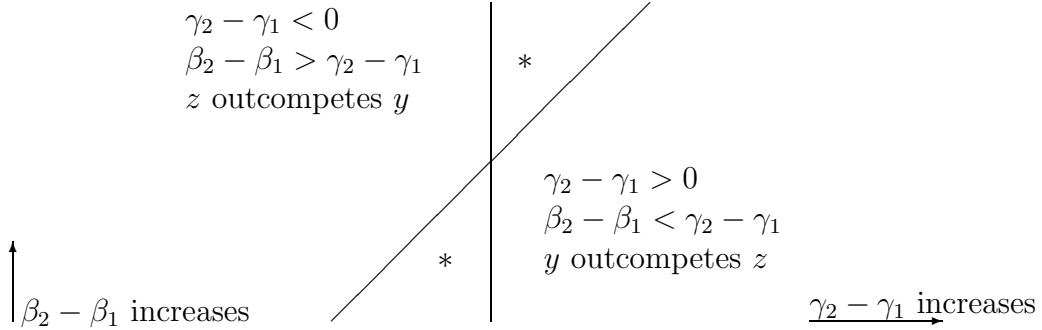


Figure 1: Validity region of Theorem 2. Competitive exclusion might be violated in the $*$ -marked regions despite the global stability principle in Theorem 3. The reasons are discussed in the subsequent sections.

strains were assumed to have different contact rates β_i , $i = 1, 2$ and different recovery rates γ_i , $i = 1, 2$. The following theorem grants competitive exclusion (cf. Hardin(1960)) regardless of stable or oscillatory dynamics.

Theorem 2. *If $\gamma_2 - \gamma_1 > 0$ and $\beta_2 - \beta_1 < \gamma_2 - \gamma_1$, then y outcompetes z in (7).*

Proof. The formula for the derivative of a quotient gives

$$d\frac{\frac{y(t)}{z(t)}}{dt} = \frac{y\psi_1(x)z - z\psi_2(x)y}{z^2} = \frac{y}{z}(\psi_1(x) - \psi_2(x)) = \frac{y}{z}((\beta_1 - \beta_2)x - (\gamma_1 - \gamma_2)).$$

We compute

$$\begin{aligned} (\psi_1 - \psi_2)(0) &= -\gamma_1 + \gamma_2 > 0 \\ (\psi_1 - \psi_2)(1) &= \beta_1 - \gamma_1 - \beta_2 + \gamma_2 > 0. \end{aligned}$$

The conditions of the theorem grant $(\psi_1 - \psi_2)(x) > 0$ for all $x \in [0, 1]$. The reason is that $\psi_1 - \psi_2$ is an affine function. Hence y/z increases along solutions of (7). Bounded proportions gives that z must tend to zero. \square

The competitive exclusion region can easily be visualized in the $(\beta_2 - \beta_1) - (\gamma_2 - \gamma_1)$ -plane, see Figure 1.

Model (7) has either one, two, or three equilibria. The disease-free equilibrium always exists at $(1, 0, 0)$. It is the only equilibrium if

$$x_1 = \frac{\gamma_1 + \lambda}{\beta_1} \geq 1, \text{ and } x_2 = \frac{\gamma_2 + \lambda}{\beta_2} \geq 1.$$

In this case, the disease-free equilibrium is globally asymptotically stable since we have $dy/dt \leq 0$ and $dz/dt \leq 0$ for valid proportions and it is the only invariant set in the domains $dy/dt = 0$ and $dz/dt = 0$, respectively. Additional endemic equilibria exist at $(x_1, F_1(x_1), 0)$ when $0 < x_1 < 1$ and at $(x_2, 0, F_2(x_2))$ when $0 < x_2 < 1$. We note that if the conditions of Theorem 2 hold, then $\psi_1 - \psi_1$ must be positive at a neighborhood of $[x_1, x_2]$ and as stated, grant competitive exclusion in equilibrium conditions. It is possible to prove more and indeed, the following global stability theorem holds.

Theorem 3. *Assume that $x_1 < \min(x_2, 1)$. Then the endemic equilibrium $(x_1, F_1(x_1), 0)$ is globally asymptotically stable in the positive octant and the positive xy -plane for (7).*

Proof. Consider the Lyapunov function (cf. Lindström (1994))

$$W(x, y, z) = x_2 \left(\int_{x_1}^x \frac{\psi_1(x')}{f_1(x')} dx' + \int_{F_1(x_1)}^{y'} \frac{y' - F_1(x_1)}{y'} dy' \right) + x_1 \int_0^z dz'. \quad (8)$$

We compute

$$\begin{aligned} \dot{W} &= x_2 \psi_1(x)(F_1(x) - y) - x_2 \frac{\psi_1(x)}{f_1(x)} f_2(x)z + x_2(y - F_1(x_1))\psi_1(x) + x_1 z \psi_2(x) \\ &= x_2 \psi_1(x)(F_1(x) - F_1(x_1)) - x_2 \frac{\psi_1(x)}{f_1(x)} f_2(x)z + x_1 z \psi_2(x) \\ &= x_2 \psi_1(x)(F_1(x) - F_1(x_1)) + \frac{z}{f_1(x)} (x_1 \psi_2(x) f_1(x) - x_2 f_2(x) \psi_1(x)) \\ &= x_2 \psi_1(x)(F_1(x) - F_1(x_1)) + \frac{z \beta_1 \beta_2 x}{f_1(x)} (x_1(x - x_2) - x_2(x - x_1)) \\ &= x_2 \psi_1(x)(F_1(x) - F_1(x_1)) + \frac{z \beta_1 \beta_2 x^2}{f_1(x)} (x_1 - x_2) \leq 0 \end{aligned}$$

The last inequality holds since F_1 is decreasing. Global stability follows by LaSalle's (1960) invariance theorem. \square

Remark 1. It follows that the endemic equilibrium $(x_2, 0, F_2(x_2))$ is globally asymptotically stable in the positive octant and the positive xz -plane if $x_2 < \min(x_1, 1)$ for (7) by the same argument.

Our analysis could end at this point since all qualitative properties of the deterministic system (7) are now known. We know that evolution selects the strain minimizing x_i , $i = 1, 2$ and that competitive exclusion follows. We shall, however, see that the global stability theorem above is not sufficient for granting neither competitive exclusion nor exclusion of oscillations. Precisely as rare violations of the competitive exclusion principle might exist (Lindström (1999) and references therein), violations could in principle exist here. Deterministic violations can, however, never occur since global stability of the endemic equilibrium has been proved and subsequent waves of the disease should decrease in amplitude with respect to the distance measure defined by the Lyapunov function (8).

5 Dimensionless parameters for the model

An important conclusion of the previous section was that it suffices to consider the two-dimensional system

$$\begin{aligned}\frac{dx}{dt} &= \lambda - \lambda x - \beta xy = \beta x \left(\frac{\lambda(1-x)}{\beta x} - y \right) = f(x)(F(x) - y), \\ \frac{dy}{dt} &= \beta xy - \gamma y - \lambda y = y\beta \left(x - \frac{\gamma + \lambda}{\beta} \right) = y\psi(x),\end{aligned}\tag{9}$$

and remember the information that evolution tends to maximize the dimensionless parameter

$$\rho_0 = \frac{\beta}{\lambda + \gamma}$$

in most cases. An important dimensionless quantity in epidemiological models is R_0 , the basic reproduction number. In (1), it is defined by

$$R_0 = \frac{\beta}{\gamma + \mu} = \beta \cdot \frac{1}{\gamma + \mu}.$$

Taking expectations of the exponential distribution gives that the expected time infected individuals remain infected in the modeled population is given

by $1/(\gamma + \mu)$. They can either be removed by natural death or by recovery and these two processes occur independently from each other. If disease control measures are applied, the recovery rate may be increased by quarantine since individuals in quarantine act dynamically as the recovered ones. As already stated in Section 1, the parameter R_0 is the product of the contact rate and the time an infected individual spends in the population. It describes the number of secondary infections that an infected individual causes in an entirely susceptible population. In (1), infected individuals are either removed by natural death or by recovery and these two processes occur independently from each other on an infinite-decimal time-scale. Contact tracing and quarantine restrictions increase the recovery rate by removing infected individuals from the population.

Putting $R_0 > 1$ implies that the number of infected individuals increases in a susceptible population. This may not be the same as requiring that the proportion of infected individuals increases. We introduce the dimensionless parameters ρ_0 and $\underline{x} = \lambda/\beta$ and time $\tau = \beta t$ in order to obtain the dimensionless model

$$\begin{aligned} x' &= x \left(\frac{1-x}{x} - y \right), \\ y' &= y \left(x - \frac{1}{\rho_0} \right). \end{aligned} \quad (10)$$

We conclude that the inequality $\rho_0 > 1$ ensures that the proportion of infected individuals increases in a population consisting of susceptible individuals. It depends on the birth rate, the contact rate, and the recovery rate. This is the parameter that we usually control as long as no vaccine is available. All mitigation measures that have an impact on R_0 does have an impact on ρ_0 , too. The contact rate is controlled by reducing the number of social contacts and the recovery rate is controlled by quarantine measures and contact tracing, i.e., possibly infected individuals are removed from the population. Minimizing the contact rate has an impact on the dynamics that the specific mitigation measure of increasing the recovery rate does not have: it increases the proportion of individuals \underline{x} in the population that is not infected at the same time. One case with $\rho_0 \leq 1$ is illustrated in Figure 2(a) and one case with $\rho_0 > 1$ is illustrated in Figure 2(b).

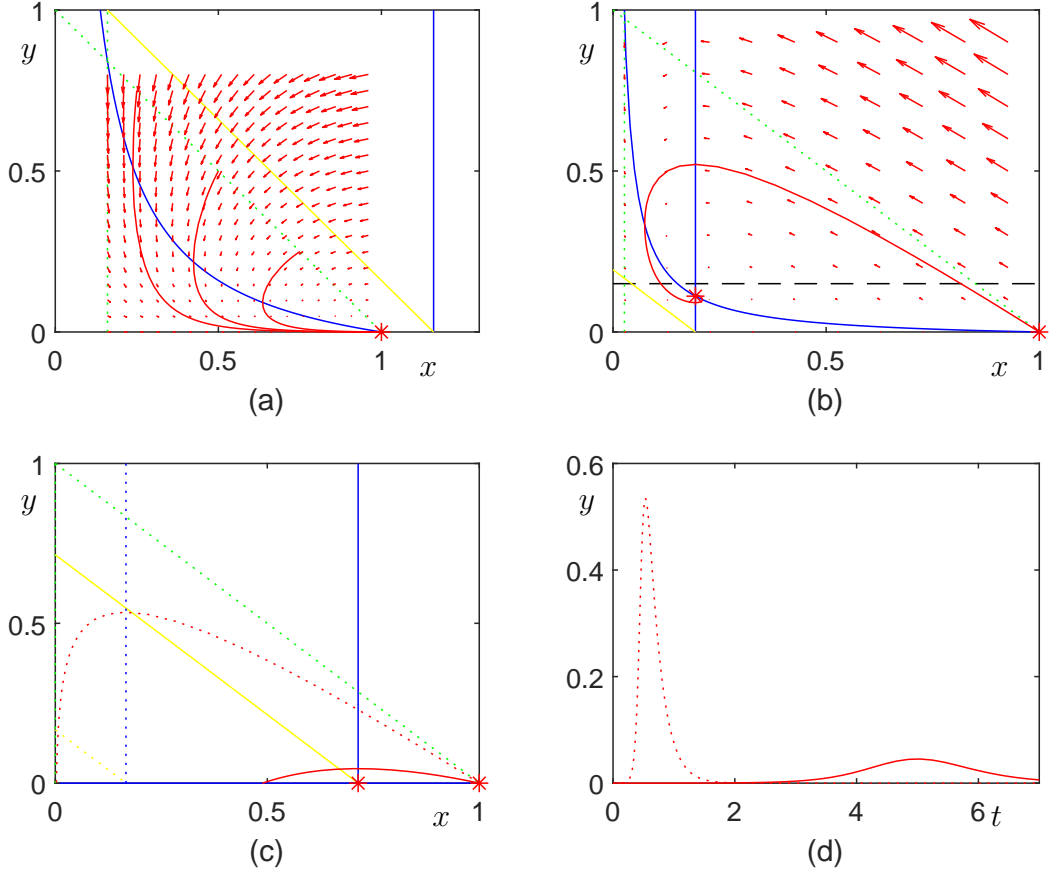


Figure 2: (a) The disease-free equilibrium of (10) is globally asymptotically stable for $\lambda = .8$, $\beta = 5$, and $\gamma = 5$. The herd-immunity region (yellow triangle) is automatically approached and the herd-immunity concept is irrelevant. (b) The endemic equilibrium of (10) is globally asymptotically stable for $\lambda = .8$, $\beta = 30$, and $\gamma = 5$. The herd-immunity region (yellow triangle) is not a domain of attraction but might be occasionally approached. The herd-immunity concept does not make sense. (c) The epidemic in (11) exhausts almost the whole population for $\lambda = 0$, $\beta = 30$, and $\gamma = 5$ (dotted red curve) whereas approximately half of the population is affected after the epidemic for $\lambda = 0$, $\beta = 7$, and $\gamma = 5$ (solid red curve). Corresponding herd-immunity regions (dotted and solid yellow triangles) are approached, but the model is not structurally stable. (d) The proportion of infected individuals against time for $\lambda = 0$, $\beta = 30$, and $\gamma = 5$ (dotted red curve) and for $\lambda = 0$, $\beta = 7$, and $\gamma = 5$ (solid red curve).

6 On realistic parameter values and their proportions

Is there any reason to continue an analysis of (10) at a stage when we know how its parameters evolve with evolution and all its qualitative properties are known? Assume now that the birth rate λ remains much smaller than the parameters related to disease transmission. These are the contact rate β and the recovery rate γ . We start checking the case $\lambda = 0$. In this case we get $\rho_0 = \beta/\gamma$ and $\underline{x} = 0$. Our system (10) takes the form

$$\begin{aligned} x' &= -xy, \\ y' &= y \left(1 - \frac{1}{\rho_0} \right). \end{aligned} \quad (11)$$

The problem with this model is that it ceases to be structurally stable (Guckenheimer and Holmes (1983)). That is, the results may be sensitive to the assumptions made in the model. A maximum for the proportion of infected individuals occurs for $x = \gamma/\beta = 1/\rho_0$. If $1/\rho_0$ is just slightly below 1 then we may call the proportion $1 - 1/\rho_0$ the excess density as in Kermack and McKendrick (1927) and we note that in this case the proportion of the population affected by the disease in the end of the epidemics is approximately the double of the excess (cf. solid red phase curve in Figure 2(c) and solid red epidemic curve in Figure 2(d)). Therefore, it is a classical result that social distancing measures reducing the contact rate and quarantine measures removing the infected proportion of individuals from the population mitigates the consequences of any epidemic. These measures do not just flatten the epidemic curve in order to save healthcare efforts but they also save a substantial part of the population from coming in contact with the disease at all. If $1/\rho_0$ is close to zero then a very large proportion of the population will be affected (cf. dotted red phase curve in Figure 2(c) and dotted red epidemic curve in Figure 2(d)). The reason for that the solid red epidemic curve develops slower in Figure 2(d) than the dotted epidemic curve is in Figure 2(c): The solid curve remains closer to the equilibria at the horizontal axis of (11) and the system is continuous.

The birth rate is certainly not zero but it is in many cases a very small quantity in comparison to the contact rate and the recovery rate. We therefore, assume that $0 < \mu < \lambda \ll \gamma < \beta$. We keep the natural death rate in this important assumption since it will reappear in the stochastic version of

the model. The last inequality is satisfied in the most interesting case $\rho_0 > 1$. The equilibrium proportion of infected individuals is then given by

$$y_* = \underline{x}(\rho_0 - 1) = \frac{\lambda}{\beta} \left(\frac{\beta}{\lambda + \gamma} - 1 \right).$$

With $\lambda \approx 0$ the equilibrium proportion of infected individuals is a very small proportion. If the population is isolated at an island it might consist of just a few individuals. The more isolated the population is, the less valid the differential equation model (1) is and a modeling technique based on stochastic processes like the one mentioned (3) and Bailey (1964) is far more appropriate. The assumption of non-zero birth rates change the epidemic curves in Figure 2(d) considerably. A lower level of mitigation measures has the consequence that the proportion of infected individuals establishes itself at a considerably higher level after the first wave, see Figure 3(a). Since the hyperbola in Figures 2(a)-(b) is strictly decreasing for positive birth rates, the equilibrium value for the proportion of infected individuals increases with relaxed mitigation measures, an observation that was quite clear in the case of Sweden in comparison to its neighboring countries during the CoViD-19 pandemic. Although the birth rate remains negligible in comparison to the disease parameters, assuming zero birth rates will hide such information.

7 On the stochastic formulation

We now formulate the stochastic version of

$$\begin{aligned} \dot{S} &= \lambda N - \beta S \frac{I}{N} - \mu S, \\ \dot{I} &= \beta S \frac{I}{N} - \gamma I - \mu I, \\ \dot{R} &= \gamma I - \mu R, \end{aligned} \tag{12}$$

and let $q_{S,I,R}$ denote the probability that the number of susceptible is S , the number of infected is I and the number of recovered is R . We keep in mind that evolution tends to maximize $\rho_0 = \beta/(\lambda + \gamma)$ in most cases as long as no physiological bound is met. The differential equations for these probabilities

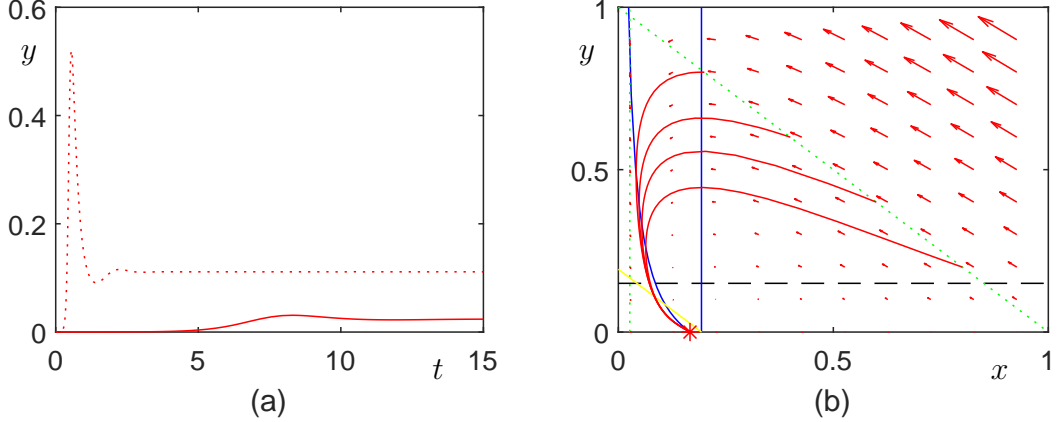


Figure 3: (a) The proportion of infected individuals against time for $\lambda = .8$, $\beta = 30$, and $\gamma = 5$ (dotted red curve) and for $\lambda = .8$, $\beta = 7$, and $\gamma = 5$ (solid red curve). (b) A sufficient vaccination as is the case for $\lambda = .8$, $\beta = 30$, $\gamma = 5$, and $\omega = 4$ ensures a globally stable equilibrium in the herd immunity region.

then read

$$\begin{aligned}
\dot{q}_{S,I,R} &= +\mu((S+1)q_{S+1,I,R} + (I+1)q_{S,I+1,R} + (R+1)q_{S,I,R+1}) \\
&\quad -\mu(S+I+R)q_{S,I,R} + \lambda(S+I+R-1)q_{S-1,I,R} \\
&\quad -\lambda(S+I+R)q_{S,I,R} + \gamma(I+1)q_{S,I+1,R} - \gamma I q_{S,I,R} \\
&\quad +\beta(S+1)\frac{I-1}{S+I+R}q_{S+1,I-1,R} - \beta S\frac{I}{S+I+R}q_{S,I,R}, \\
&\quad S = 1, 2, \dots, I = 1, 2, \dots, R = 0, 1, 2, \dots \\
\dot{q}_{0,I,R} &= +\mu(q_{1,I,R} + (I+1)q_{0,I+1,R} + (R+1)q_{0,I,R+1}) - \mu(I+R)q_{0,I,R} \\
&\quad -\lambda(I+R)q_{0,I,R} + \gamma(I+1)q_{0,I+1,R} - \gamma I q_{0,I,R} \\
&\quad +\beta\frac{I-1}{I+R}q_{1,I-1,R}, \quad S = 0, \quad I = 1, 2, \dots, \quad R = 0, 1, 2, \dots \quad (13) \\
\dot{q}_{S,0,R} &= +\mu((S+1)q_{S+1,0,R} + q_{S,1,R} + (R+1)q_{S,0,R+1}) \\
&\quad -\mu(S+R)q_{S,0,R} + \lambda(S+R-1)q_{S-1,0,R} \\
&\quad -\lambda(S+R)q_{S,0,R} + \gamma q_{S,1,R}, \quad S = 1, 2, \dots, \quad I = 0, \quad R = 0, 1, 2, \dots \\
\dot{q}_{0,0,R} &= +\mu(q_{1,0,R} + q_{0,1,R} + (R+1)q_{0,0,R+1}) \\
&\quad -\mu R q_{0,0,R} - \lambda R q_{0,0,R} + \gamma q_{0,1,R}, \quad S = 0, \quad I = 0, \quad R = 0, 1, 2, \dots
\end{aligned}$$

and we implemented these equations for simulation studies in order to find out the dependence of the size of the population on the results. Before a simulation study is made, one need to check that the equations meet as many conditions as possible in limiting cases. We start with the following theorem.

Theorem 4. *The total probability $\sum_{S=0}^{\infty} \sum_{I=0}^{\infty} \sum_{R=0}^{\infty} q_{S,I,R}$ is an invariant for (13) and the contribution to changes in the total probability that are related to each of the parameters is zero.*

The proof of this theorem contains basically the techniques alluded to in Lemma 1 and is given in Appendix A. We also conclude that extinction of the infection is an absorbing state and that extinction of the population is an absorbing state within that state. Also, here the proof follows standard techniques and is given in Appendix B.

Theorem 5. *The probabilities $q_{0,0,0}$ and $\sum_{S=0}^{\infty} \sum_{R=0}^{\infty} q_{S,0,R}$ increase with time.*

The birth-death processes of model (13) coincide with those of the birth-death model (3). Therefore, solutions of (13) coincide with the known solutions (4) of (3) in a limiting case. This is an important part of the validation of the numerical version of (13).

Typical simulation results are given in Figure 4. We use $\lambda = .0051$, $\mu = .005$, $\gamma = .2$, and $\beta = 1.5$ to illustrate a typical outcome and the initial conditions are $S(0) = 209$, $I(0) = 1$, and $R(0) = 0$. This selection gives rise to just negligible probabilities corresponding to population sizes above 300 as long as we limit the simulation to the time interval $0 \leq t \leq 200$. Our numerical model for (3) contains 4,545,100 equations as this size limit is applied. This allowed for completing the simulation on a laptop during a few days without encountering memory problems.

The thin green curve on the top of the diagram illustrates the \log_{10} -value of the survival probability of the population indicating that probability of survival for the population is almost 1. The thick green curve illustrates the \log_{10} -value of the probability of survival of the infection. This probability drops rapidly after $t = 150$ which makes it hard to do particular simulations of (13) that last longer than this. The expectations of the proportions of the susceptible individuals, infected individuals, and recovered individuals are given by solid curves in blue, red, and yellow, respectively. These values have no tendency to show oscillatory behavior and we expect that this

behavior to be even more robust for larger populations that have more valid diffusion approximations, see e. g. Allen (2008). Possible instabilities have therefore, not their origin in the time-dependent probabilities the model (13) themselves.

We illustrated the corresponding proportions that were predicted by the deterministic model (12) with dashed curves in corresponding colors in the same diagram. According to Theorem 3, they predict damped oscillations. One particular simulation (13) up to extinction of the disease is indicated by dotted curves in the corresponding colors. In general, extinction of the disease occurs before the drop in the survival probability of the disease takes place after $t = 150$. We conclude that the fluctuations especially in the fraction of infected individuals are quite violent before extinction of the disease. This indicates that the instability is a feature of the particular realizations of orbits and not the probability distributions that act as solutions to (13). In Figure 5 we dropped the simulations of the probabilities of (13) for a case where the model has grown out of bounds. Here we have $\lambda = .0051$, $\mu = .005$, $\gamma = .2$, and $\beta = 1.5$ but now the initial conditions are $S(0) = 1499$, $I(0) = 1$, and $R(0) = 0$. But we still simulated particular simulations up to extinction with dotted curves and solutions of the deterministic model (12) with dashed curves. Because of the larger population, the infection is less prone to go extinct and in many cases, we can continue the simulation at least until $t = 1000$. We note that oscillations in the population of infected individuals remain after that solution of (12) has been stabilized in the vicinity of the endemic equilibrium.

8 Vaccination and herd-immunity

We have so far considered (A) social distancing measures basically changing the contact rate β , (B) quarantine and contact tracing measures removing possible infective individuals by changing the recovery (or removal) rate γ , and (C) travel restriction measures isolating some part of the population. In terms of model (7) the measures (A) and (B) are both equivalent to a change in ρ_0 whereas the measure (C) hits at the long-run tendency that an epidemic will affect a quite small proportion of the population consisting of just a few individuals if the population remains isolated enough. Subsequent longer periods giving support for not more than a few infected individuals in the population increases the probability of extinction of the disease rapidly.

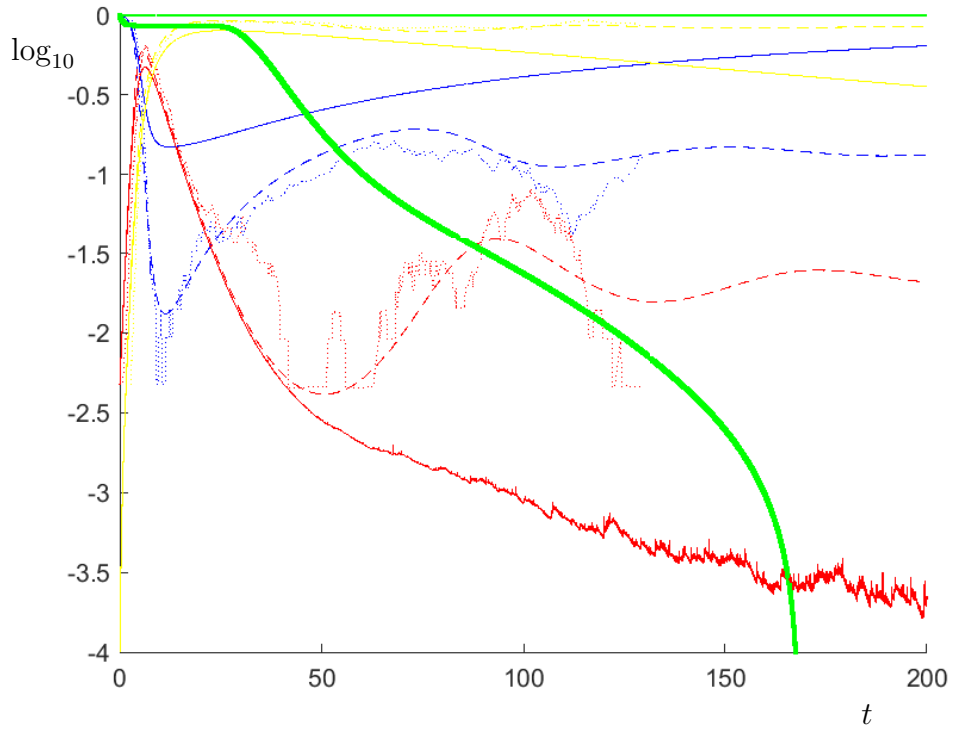


Figure 4: \log_{10} values of either proportions or probabilities. Model (13) is compared to its deterministic counterpart (12) and the parameters are $\lambda = .0051$, $\mu = .005$, $\gamma = .2$, and $\beta = 1.5$. The initial conditions are $S(0) = 209$, $I(0) = 1$, and $R(0) = 0$. The thin and thick green curves are the survival probabilities of the population and the infection, respectively. The solid blue, red, and yellow curves are the expected proportions of susceptible, infected and recovered individuals according to (13). The dashed curves are the corresponding simulation of the deterministic model (12). A particular realization of an outcome from model (13) is given by the dotted curves.

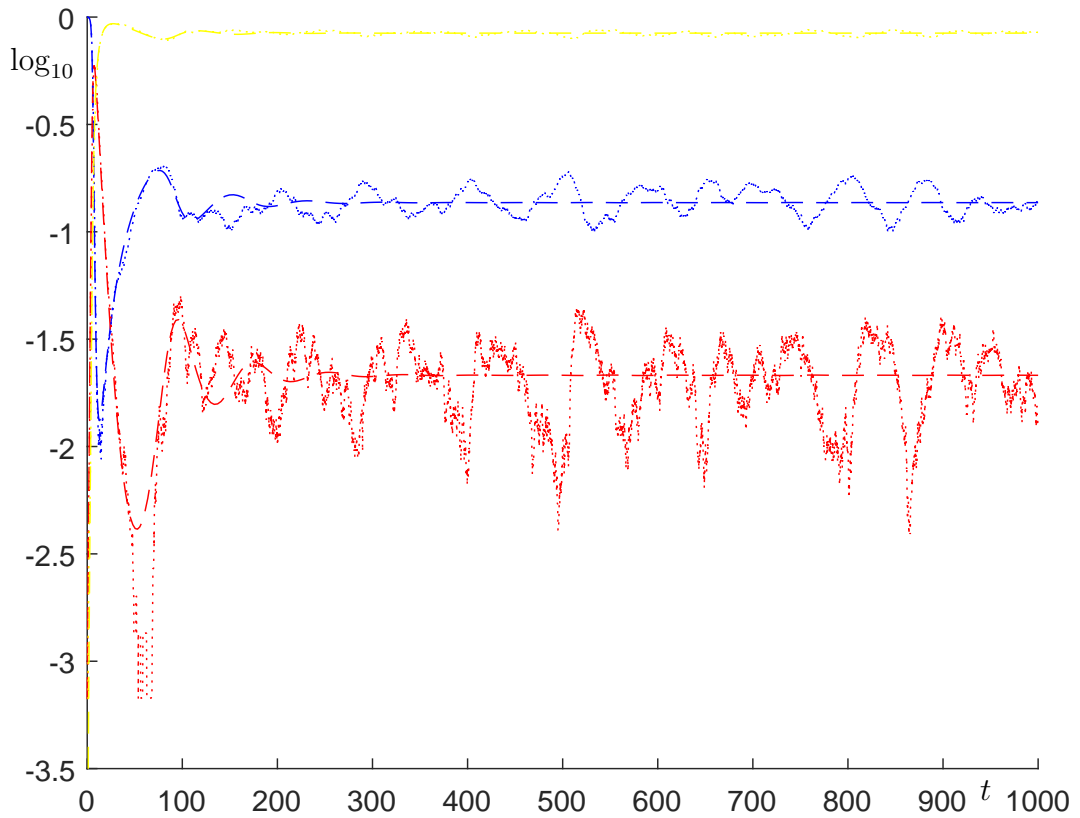


Figure 5: \log_{10} values of proportions of susceptible, infected, and recovered individuals as predicted by (13) (dotted) and (12) (dashed). Parameters used are $\lambda = .0051$, $\mu = .005$, $\gamma = .2$, and $\beta = 1.5$ and the used initial conditions are $S(0) = 1499$, $I(0) = 1$, and $R(0) = 0$. It does not make sense to simulate probability distributions of (13) because any valid numerical model becomes far too large. The dashed curves are the corresponding simulation of the deterministic model (12). A particular realization of an outcome from model (13) is given by the dotted curves.

We now add a vaccination rate ω to (7) and get

$$\begin{aligned}\frac{dx}{dt} &= \lambda - \lambda x - \omega x - \beta xy = \beta x \left(\frac{(\lambda + \omega) \left(\frac{\lambda}{\lambda + \omega} - x \right)}{\beta x} - y \right), \\ \frac{dy}{dt} &= \beta xy - \gamma y - \lambda y = \beta y \left(x - \frac{\gamma + \lambda}{\beta} \right).\end{aligned}$$

Also here, we introduce the dimensionless parameters

$$\underline{x} = \frac{\lambda + \omega}{\beta}, \hat{x} = \frac{\lambda}{\lambda + \omega}, \rho_0 = \frac{\beta}{\gamma + \lambda},$$

and get with respect to dimensionless time

$$\begin{aligned}\dot{x} &= x \left(\underline{x} \frac{\hat{x} - x}{x} - y \right), \\ \dot{y} &= y \left(x - \frac{1}{\rho_0} \right).\end{aligned}\tag{14}$$

The model (14) still possesses the same global stability properties as (10) and techniques in the proof of Theorem 3 can still be applied step-by-step. The endemic equilibrium is globally asymptotically stable when a hyperbola (the susceptible isocline) intersects a vertical line (the infective isocline) in the interior of compact triangle specified by Theorem 1. Social distancing measures (A) and quarantine and contact tracing measures (B) both shifted the vertical line to the right but vaccination will shift the hyperbola to the left and will introduce a possibility to remove the disease by forming a globally stable equilibrium inside the herd immunity region

$$x \geq 0, y \geq 0, x + y \leq \frac{1}{\rho_0},$$

see Figure 3(b). Such a possibility does not exist without vaccination. In fact, the herd immunity region is never defined if social distancing measures, quarantine measures, or contact tracing measures are used since they all change ρ_0 . In the case of natural transmission, the concept of herd immunity is either irrelevant (Figure 2(a)), not well-defined or not in a domain of attraction (Figure 2(b)), or sensitive to modeling errors and structural instability (Figure 2(c)).

9 Summary

Much confusion about epidemic models have been prevailing over decades and we think it is time to describe the mechanism that is responsible for the transition between stochastic and deterministic behavior in such models.

Our assumption of an exponential growth of the population and the fact that population parameters like natural birth and death operate on a slower time-scale than disease parameters like contact and recovery rates ensures that globally stable endemic equilibria correspond to low proportions of infected individuals. Low proportions of individuals correspond to low numbers of individuals if the population is isolated or small. These low proportions decrease with increased pre-vaccination mitigation measures aiming at control of the infectiousness of the disease.

Low asymptotic average proportions constitute a mechanism for a transition from primary deterministic dynamics to stochastic dynamics. Subsequent waves start therefore, usually as local outbreaks at seemingly randomly selected places.

Our description in terms of proportion makes another result clear, too. If several strains are assumed to compete against each other and the proportion of susceptible remains in the vicinity of the proportion of susceptible of an endemic equilibrium, then the strain with the highest ability to increase its proportion will outcompete all other strains. The expected effect of this evolution theorem is that the contact rate first increases until some physiological bound is reached. After this, the pathogen attempts to slow down the recovery or removal rate by avoiding virulence and quarantine measures.

The stochastic formulation of the model includes the possibility of extinction of both the population and the disease. If the size of the population is small, such probabilities are usually high. Diseases can go extinct on isolated islands. We remind the reader that during the CoViD-19 epidemic the disease was easier to get under control at societies with easily controlled boarders (Iceland, Taiwan, Oceania, New Zealand, Australia, Japan, South Korea). The smaller society, the less sensitive the result was to the set of mitigation strategies actually applied.

The smaller the unit with easily controlled boarders is, the larger the probability of extinction. As soon as the population size is large enough to keep the probability of extinction low, oscillatory patterns that are not present in the deterministic model become visible. It is therefore essential to implement regional quarantine measures as soon as local outbreaks are

observed.

The probability distributions of the stochastic model are not connected to any time-dependent or oscillatory patterns. They remain close enough to diffusion approximations that usually are connected to stable equilibrium solutions. Instead, it is the particular realizations of the model that display the oscillatory pattern. These oscillations might introduce violations of the competitive exclusion principle alluded to above but this is not very likely. The formulation of useful conditions for such violations remains an open problem.

We end up by a discussion of the herd-immunity concept and conclude that this concept remains without meaning in connection to pre-vaccination mitigation strategies. If we have $\rho_0 \leq 1$, then we are automatically in the herd-immunity region. The concept is irrelevant. There is no herd-immunity to be achieved. If we have $\rho_0 > 1$, then the herd-immunity region is not an attraction domain and the proportion of infected individuals will tend to remain unchanged with time. Natural transmission cannot produce herd-immunity for eradication of the disease. In addition, the objective of pre-vaccination pandemic mitigation strategies is to make ρ_0 smaller. Such measures change the herd-immunity region and introduce problems with the definition of the concept.

Finally, we comment the concept of herd-immunity in the case a disease is so infectious that it will infect almost the whole population in the first wave (Kermack and McKendrick (1927)). In this case we are close to a structurally unstable case (Guckenheimer and Holmes (1983)) and the number of infected individuals will be extremely low after the first wave, too. The probability of extinction of the disease is after such an event huge. But measles is a very infectious disease that has not been eradicated without vaccines. Indeed, measles could be practically extinct during the pre-vaccination era for many years at islands containing populations of up to some hundred thousand individuals (Cliff and Haggett (1980)).

The spectrum of phenomena that can be included in concepts like herd immunity can naturally be discussed. But we think a mess around the concept is created if we allow the concept to include phenomena that are related to population size. If herd-immunity is used then we must restrict it to relate to well-defined proportions of recovered or removed individuals only. Such criteria hold only when we are able to apply vaccination strategies successfully enough to make all other measures superfluous.

A Proof of Theorem 4

Proof. We commence by taking each of the contributions to the total change that are related to each of the involved processes separately and conclude finally that the total probability is an invariant. We begin with changes that are related to the recovery rate γ . We get

$$\begin{aligned}
& \sum_{R=0}^{\infty} q_{0,1,R} + \sum_{R=0}^{\infty} \sum_{S=1}^{\infty} q_{S,1,R} + \sum_{R=0}^{\infty} \sum_{I=1}^{\infty} (I+1)q_{0,I+1,R} - \sum_{R=0}^{\infty} \sum_{I=1}^{\infty} Iq_{0,I,R} \\
& + \sum_{R=0}^{\infty} \sum_{I=1}^{\infty} \sum_{S=1}^{\infty} (I+1)q_{S,I+1,R} - \sum_{R=0}^{\infty} \sum_{I=1}^{\infty} \sum_{S=1}^{\infty} Iq_{S,I,R} \\
= & \sum_{R=0}^{\infty} q_{0,1,R} + \sum_{R=0}^{\infty} \sum_{I=2}^{\infty} Iq_{0,I,R} - \sum_{R=0}^{\infty} \sum_{I=1}^{\infty} Iq_{0,I,R} + \sum_{R=0}^{\infty} \sum_{S=1}^{\infty} q_{S,1,R} \\
& + \sum_{R=0}^{\infty} \sum_{I=2}^{\infty} \sum_{S=1}^{\infty} Iq_{S,I,R} - \sum_{R=0}^{\infty} \sum_{I=1}^{\infty} \sum_{S=1}^{\infty} Iq_{S,I,R} = 0.
\end{aligned}$$

Therefore, the recovery process is well-formulated in the sense that it leaves the total probability invariant. Next, we take the infection process related to the contact rate β . We get

$$\begin{aligned}
& \sum_{R=0}^{\infty} \sum_{I=1}^{\infty} \frac{I-1}{I+R} q_{1,I-1,R} + \sum_{R=0}^{\infty} \sum_{I=1}^{\infty} \sum_{S=1}^{\infty} \frac{(S+1)(I-1)}{S+I+R} q_{S+1,I-1,R} \\
& - \sum_{R=0}^{\infty} \sum_{I=1}^{\infty} \sum_{S=1}^{\infty} \frac{SI}{S+I+R} q_{S,I,R} \\
= & \sum_{R=0}^{\infty} \sum_{I=1}^{\infty} \frac{I}{1+I+R} q_{1,I,R} + \sum_{R=0}^{\infty} \sum_{I=1}^{\infty} \sum_{S=2}^{\infty} \frac{SI}{S+I+R} q_{S,I,R} \\
& - \sum_{R=0}^{\infty} \sum_{I=1}^{\infty} \sum_{S=1}^{\infty} \frac{SI}{S+I+R} q_{S,I,R} = 0
\end{aligned}$$

so the infection process has the same property. We then check the invariance property for the birth process. We get

$$\begin{aligned}
& - \sum_{R=0}^{\infty} R q_{0,0,R} - \sum_{S=1}^{\infty} \sum_{R=0}^{\infty} (S+R) q_{S,0,R} + \sum_{S=1}^{\infty} \sum_{R=0}^{\infty} (S+R-1) q_{S-1,0,R} \\
& - \sum_{I=1}^{\infty} \sum_{R=0}^{\infty} (I+R) q_{0,I,R} - \sum_{S=1}^{\infty} \sum_{I=1}^{\infty} \sum_{R=0}^{\infty} (S+I+R) q_{S,I,R} \\
& + \sum_{S=1}^{\infty} \sum_{I=1}^{\infty} \sum_{R=0}^{\infty} (S+I+R-1) q_{S-1,I,R} \\
= & - \sum_{R=0}^{\infty} R q_{0,0,R} - \sum_{S=1}^{\infty} \sum_{R=0}^{\infty} (S+R) q_{S,0,R} + \sum_{S=0}^{\infty} \sum_{R=0}^{\infty} (S+R) q_{S,0,R} \\
& - \sum_{I=1}^{\infty} \sum_{R=0}^{\infty} (I+R) q_{0,I,R} - \sum_{S=1}^{\infty} \sum_{I=1}^{\infty} \sum_{R=0}^{\infty} (S+I+R) q_{S,I,R} \\
& + \sum_{S=0}^{\infty} \sum_{I=1}^{\infty} \sum_{R=0}^{\infty} (S+I+R) q_{S,I,R} = 0
\end{aligned}$$

so the birth process meets the invariance requirement. The death process governed by the parameter μ remains. We get

$$\begin{aligned}
& - \sum_{R=0}^{\infty} R q_{0,0,R} + \sum_{R=0}^{\infty} (R+1) q_{0,0,R+1} + \sum_{R=0}^{\infty} q_{0,1,R} + \sum_{R=0}^{\infty} q_{1,0,R} \\
& - \sum_{S=1}^{\infty} \sum_{R=0}^{\infty} (S+R) q_{S,0,R} + \sum_{S=1}^{\infty} \sum_{R=0}^{\infty} (R+1) q_{S,0,R+1} + \sum_{S=1}^{\infty} \sum_{R=0}^{\infty} q_{S,1,R} \\
& + \sum_{S=1}^{\infty} \sum_{R=0}^{\infty} (S+1) q_{S+1,0,R} - \sum_{I=1}^{\infty} \sum_{R=0}^{\infty} (I+R) q_{0,I,R} + \sum_{I=1}^{\infty} \sum_{R=0}^{\infty} (R+1) q_{0,I,R+1} \\
& + \sum_{I=1}^{\infty} \sum_{R=0}^{\infty} (I+1) q_{0,I+1,R} + \sum_{I=1}^{\infty} \sum_{R=0}^{\infty} q_{1,I,R} - \sum_{S=1}^{\infty} \sum_{I=1}^{\infty} \sum_{R=0}^{\infty} (S+I+R) q_{S,I,R} \\
& + \sum_{S=1}^{\infty} \sum_{I=1}^{\infty} \sum_{R=0}^{\infty} (R+1) q_{S,I,R+1} + \sum_{S=1}^{\infty} \sum_{I=1}^{\infty} \sum_{R=0}^{\infty} (I+1) q_{S,I+1,R} \\
& + \sum_{S=1}^{\infty} \sum_{I=1}^{\infty} \sum_{R=0}^{\infty} (S+1) q_{S+1,I,R}
\end{aligned}$$

which equals

$$\begin{aligned}
& - \sum_{R=0}^{\infty} Rq_{0,0,R} + \sum_{R=1}^{\infty} Rq_{0,0,R} + \sum_{R=0}^{\infty} q_{0,1,R} + \sum_{R=0}^{\infty} q_{1,0,R} \\
& - \sum_{S=1}^{\infty} \sum_{R=0}^{\infty} Sq_{S,0,R} - \sum_{S=1}^{\infty} \sum_{R=0}^{\infty} Rq_{S,0,R} + \sum_{S=1}^{\infty} \sum_{R=1}^{\infty} Rq_{S,0,R} + \sum_{S=1}^{\infty} \sum_{R=0}^{\infty} q_{S,1,R} \\
& + \sum_{S=2}^{\infty} \sum_{R=0}^{\infty} Sq_{S,0,R} - \sum_{I=1}^{\infty} \sum_{R=0}^{\infty} Iq_{0,I,R} - \sum_{I=1}^{\infty} \sum_{R=0}^{\infty} Rq_{0,I,R} + \sum_{I=1}^{\infty} \sum_{R=1}^{\infty} Rq_{0,I,R} \\
& + \sum_{I=2}^{\infty} \sum_{R=0}^{\infty} Iq_{0,I,R} + \sum_{I=1}^{\infty} \sum_{R=0}^{\infty} q_{1,I,R} - \sum_{S=1}^{\infty} \sum_{I=1}^{\infty} \sum_{R=0}^{\infty} Sq_{S,I,R} \\
& - \sum_{S=1}^{\infty} \sum_{I=1}^{\infty} \sum_{R=0}^{\infty} Iq_{S,I,R} - \sum_{S=1}^{\infty} \sum_{I=1}^{\infty} \sum_{R=0}^{\infty} Rq_{S,I,R} + \sum_{S=1}^{\infty} \sum_{I=1}^{\infty} \sum_{R=1}^{\infty} Rq_{S,I,R} \\
& + \sum_{S=1}^{\infty} \sum_{I=2}^{\infty} \sum_{R=0}^{\infty} Iq_{S,I,R} + \sum_{S=2}^{\infty} \sum_{I=1}^{\infty} \sum_{R=0}^{\infty} Sq_{S,I,R} = 0.
\end{aligned}$$

We have proved that the total probability is an invariant with respect to time and that the contribution of each of the processes to changes in the total probability is zero. \square

B Proof of Theorem 5

Proof. We have

$$\frac{dq_{0,0,0}}{dt} = \mu(q_{1,0,0} + q_{0,1,0} + q_{0,0,1}) + \gamma q_{0,1,0} \geq 0$$

meaning that the probability of extinction of the population increase with time and

$$\begin{aligned}
\sum_{S=0}^{\infty} \sum_{R=0}^{\infty} \frac{dq_{S,0,R}}{dt} &= \mu \sum_{R=0}^{\infty} q_{1,0,R} + \mu \sum_{R=0}^{\infty} q_{0,1,R} + \mu \sum_{R=0}^{\infty} (R+1) q_{0,0,R+1} \\
&\quad - \mu \sum_{R=0}^{\infty} R q_{0,0,R} - \lambda \sum_{R=0}^{\infty} R q_{0,0,R} + \gamma \sum_{R=0}^{\infty} q_{0,1,R} \\
&\quad + \mu \sum_{S=1}^{\infty} \sum_{R=0}^{\infty} (S+1) q_{S+1,0,R} + \mu \sum_{S=1}^{\infty} \sum_{R=0}^{\infty} q_{S,1,R} \\
&\quad + \mu \sum_{S=1}^{\infty} \sum_{R=0}^{\infty} (R+1) q_{S,0,R+1} - \mu \sum_{S=1}^{\infty} \sum_{R=0}^{\infty} (S+R) q_{S,0,R} \\
&\quad + \lambda \sum_{S=1}^{\infty} \sum_{R=0}^{\infty} (S+R-1) q_{S-1,0,R} - \lambda \sum_{S=1}^{\infty} \sum_{R=0}^{\infty} (S+R) q_{S,0,R} \\
&\quad + \gamma \sum_{S=1}^{\infty} \sum_{R=0}^{\infty} q_{0,1,R} \\
&= \mu \sum_{R=0}^{\infty} q_{1,0,R} + \mu \sum_{R=0}^{\infty} q_{0,1,R} + \mu \sum_{R=1}^{\infty} R q_{0,0,R} - \mu \sum_{R=0}^{\infty} R q_{0,0,R} \\
&\quad - \lambda \sum_{R=0}^{\infty} R q_{0,0,R} + \gamma \sum_{R=0}^{\infty} q_{0,1,R} + \mu \sum_{S=2}^{\infty} \sum_{R=0}^{\infty} S q_{S,0,R} \\
&\quad + \mu \sum_{S=1}^{\infty} \sum_{R=0}^{\infty} q_{S,1,R} + \mu \sum_{S=1}^{\infty} \sum_{R=1}^{\infty} R q_{S,0,R} \\
&\quad - \mu \sum_{S=1}^{\infty} \sum_{R=0}^{\infty} (S+R) q_{S,0,R} + \lambda \sum_{S=0}^{\infty} \sum_{R=0}^{\infty} (S+R) q_{S,0,R} \\
&\quad - \lambda \sum_{S=1}^{\infty} \sum_{R=0}^{\infty} (S+R) q_{S,0,R} + \gamma \sum_{S=1}^{\infty} \sum_{R=0}^{\infty} q_{0,1,R} \\
&= \mu \sum_{R=0}^{\infty} q_{1,0,R} + \mu \sum_{S=1}^{\infty} \sum_{R=0}^{\infty} q_{S,1,R} + \gamma \sum_{S=0}^{\infty} \sum_{R=0}^{\infty} q_{0,1,R} \geq 0
\end{aligned}$$

meaning that the probability of extinction of the disease will increase with time. \square

References

- [1] L. J. S. Allen. An introduction to stochastic epidemic models. In F. Brauer, P. van den Driessche, and J. Wu, editors, *Mathematical Epidemiology*, volume 1945 of *Lecture Notes in Mathematics*. Springer, Berlin, 2008.
- [2] N. T. J. Bailey. *The Elements of Stochastic Processes*. Wiley, New York, 1964.
- [3] P. G. Barrentos, J. Ángel Rodríguez, and A. Ruiz-Herrera. Global dynamics in the seasonally forced SIR epidemic model. *Journal of Mathematical Biology*, 75:1655–1668, 2017.
- [4] A. D. Becker, A. Wesolowski, O. N. Björnstad, and B. T. Grenfell. Long-term dynamics of measles in London: Titrating the impact of wars, the 1918 pandemic and vaccination. *PLoS Comput Biol*, 15(9):e1007305, 2019.
- [5] A. D. Cliff and P. Haggett. Changes in the seasonal incidence of measles in Iceland. *The Journal of Hygiene*, 85(3):451–457, 1980.
- [6] T. C. Germann, K. Kadau, I. M. Longini, and C. A. Macken. Mitigation strategies for pandemic influenza in the United States. *Proceedings of the National Academy of Sciences of the United States of America*, 103:5935–5940, 2006.
- [7] P. Glendinning and L. Perry. Melnikov analysis of chaos in a simple epidemiological model. *Journal of Mathematical Biology*, 35:359–373, 1997.
- [8] J. Guckenheimer and P. Holmes. *Nonlinear Oscillations, Dynamical Systems, and Bifurcations of Vector Fields*. Springer-Verlag, 1983.
- [9] G. Hardin. The competitive exclusion principle. *Science*, 131:1292–1297, 1960.
- [10] M. J. Keeling, P. Rohani, and B. T. Grenfell. Seasonally forced disease dynamics explored as switching between attractors. *Physica D*, 148:317–335, 2001.

- [11] W. O. Kermack and A. G. McKendrick. A contribution to the mathematical theory of epidemics. *Proceedings of the Royal Society of London A*, 115(772):700–721, 1927.
- [12] J. P. LaSalle. Some extensions of Lyapunovs second method. *IRE Transactions of Circuit Theory*, CT-7:520–527, 1960.
- [13] T. Lindström. Global stability of a model for competing predators. In M. Gyllenberg and L.-E. Persson, editors, *Analysis, Algebra, and Computers in Mathematical Research*, pages 233–245. Marcel Dekker, Inc., New York, Basel, Hong Kong, 1994.
- [14] T. Lindström. Global stability of a model for competing predators: An extension of the the Ardito & Ricciardi Lyapunov function. *Nonlinear Analysis*, 39:793–805, 2000.
- [15] C. C. McCluskey. Complete global stability for an SIR epidemic model with delay distributed of discrete. *Nonlinear Analysis: Real World Applications*, 11(1):55–59, 2010.
- [16] L. F. Olsen and W. M. Schaffer. Chaos versus noisy periodicity: Alternative hypotheses for childhood epidemics. *Science*, 249:499–504, 1990.
- [17] H. L. Smith. *An Introduction to Delay Differential Equations with Applications to Life Sciences*. Springer, 2011.